

NUMERICAL INVESTIGATION OF MELTING PROCESS INCLUDING NATURAL CONVECTION INSIDE A RECTANGULAR ENCLOSURE HEATED BY PROTRUDING PULSED HEAT SOURCES

Brahim AMAHAN, Hamid EL QARNIA

Cadi Ayyad University, Faculty of Sciences Semlalia, Fluid Mechanics and Energetic Laboratory, Affiliate to CNRST, URAC 27, Department of Physics, P.O. 2390, Marrakesh, Morocco + Email: brahim.amahan@gmail.com

ABSTRACT

The present study explores numerically the process of melting of the phase-change material (PCM) for cooling electronic components or heat storage applications. The system studied is a rectangular enclosure filled with PCM. Three protruding generating heat sources are attached on one of the vertical walls of the enclosure, and generating heat at a pulsed form and uniform volumetric rate. The power generated in heat sources is dissipated in PCM. The advantage of using PCM is that it is able to absorb high amount of heat generated by heat sources due to its relatively high energy density. To investigate the thermal behavior and thermal performance of the proposed system, a mathematical model based on the mass, momentum and energy conservation equations was developed. After validating the proposed mathematical model against experimental data, numerical investigations were next conducted to examine the impact of the frequency of the pulsed power generated and the aspect ratio of the enclosure on the cooling capacity and energy storage of the PCM-based heat sink.

Keywords: *phase change material, melting, thermal energy storage, pulsed heating, electronic cooling.*

1. Introduction

Studying the melting of phase change materials (PCM) in a rectangular enclosure provided with discrete heat sources has been the subject of several analytical, experimental and numerical studies during recent decades. The first study describing this subject was carried out by Chu et al. [1]. The numerical study showed that the optimum position of the heat source that maximizes heat transfer is depending on the Rayleigh number. Zhang [2] have conducted an experimental study of melting of PCM (n-octadecane) inside a rectangular cavity heated by flush-mounted heat sources on one of its vertical walls at constant and uniform heat generation. The horizontal walls are adiabatic. The results obtained show that the cooling of heat sources using PCM melting natural convection leads to a drop of the mean temperatures of heat sources as much as 50% compared to air natural convection cooling (for a certain time). Binet et al. [3] have developed a (2D) mathematical model simulating the thermal behaviour of a rectangular enclosure similar to the one studied in [2].

Their study finds applications in the design of heat storage units and cooling of electronic equipments. Krishnan et al. [4] have considered the melting process of PCM in a rectangular enclosure heated by three pulsed heat sources stamped into one of the two vertical walls. The authors conducted numerical investigations to study the effect of melting process on the cooling of heat sources. The same problem has been conducted numerically by Faraji and El Qarnia [5] where the protruding heat sources simulating electronic components. Correlations have been established in terms of duration of safe operation and melting time.

To the author's knowledge, no study on the melting of PCM in a rectangular enclosure heated by pulsed protruding heat sources has been addressed. The proposed study addresses this problem numerically by performing numerical investigations of the melting of PCM in a rectangular enclosure heated by three pulsed protruding heat sources. Among the control parameters of the system studied, there is the dimensionless frequency of the pulsed power generated by each heat source. The effect of such frequency on the maximum dimensionless temperature of pulsed heat sources, the flow structure and the thermal field is examined.

2. Mathematical model and formulation

The system studied is shown schematically in Figure 1. Pulsed power density generated in the heat sources is illustrated in Figure 2.

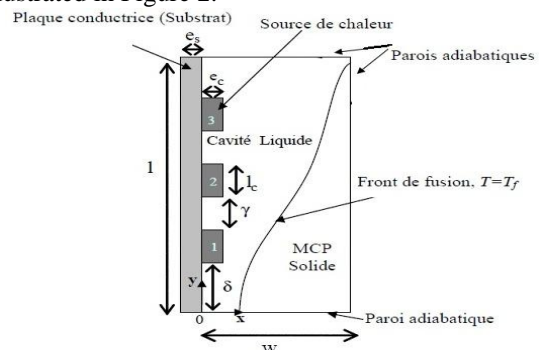


Fig.1- The schematic view of the physical model.

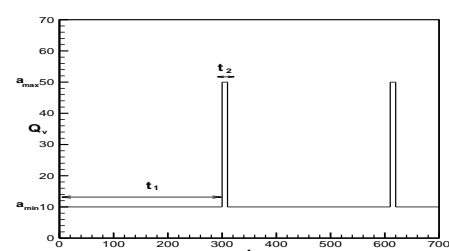


Fig. 2- Pulsed power generated in the heat sources for the first two cycles.

The times t_1 and t_2 represent the durations of minimum and maximum values of the pulsed power per unit length (10 W/m and 50 W/m).

Governing equations

In the mathematical formulation of the problem, the governing equations for mass, momentum and energy transport, boundary and initial conditions are obtained using the following dimensionless parameters:

$$X = \frac{x}{l_0}, \quad Y = \frac{y}{l_0}, \quad \tau = \frac{\alpha_{m,1}}{l_0^2} t, \quad U = \frac{u}{\alpha_{m,1}/l_0}, \quad V = \frac{v}{\alpha_{m,1}/l_0}$$

$$\Delta T = \frac{3a_{moy}}{k_{m,1}}, \quad \theta = \frac{T - T_f}{\Delta T}, \quad P_r = \frac{g}{\alpha_{m,1}}, \quad R_a = \frac{g\beta l_0^3 \Delta T}{g_{m,1} \alpha_{m,1}}$$

$$Ste = \frac{c_{ml,p} \Delta T}{\Delta H_f}, \quad P_c = \frac{l_0^2}{\alpha_{m,1}} P_e, \quad f = \frac{1}{P_c}, \quad P = \frac{P}{\rho(\alpha_{m,1}/l_0)^2}, \quad \bar{\alpha} = \frac{\alpha}{\alpha_{m,1}}$$

$$\text{With, } a_{moy} = \frac{a_{min}^* t_1 + a_{max}^* t_2}{P_c}, \quad P_c = t_1 + t_2, \quad g_{m,1} = \frac{\mu_m}{\rho_m}$$

The quantity $l_0 = \sqrt{lw - 3l_c e_c}$ is chosen as a characteristic length, and represents the reference mass of the PCM.

$$\frac{\partial U}{\partial X} + \frac{\partial V}{\partial Y} = 0 \quad (1)$$

$$\frac{\partial U}{\partial \tau} + \frac{\partial(UU)}{\partial X} + \frac{\partial(VU)}{\partial Y} = P_r \frac{\partial^2 U}{\partial X^2} + P_r \frac{\partial^2 U}{\partial Y^2} - \frac{\partial P}{\partial X} + S_U \quad (2)$$

$$\frac{\partial V}{\partial \tau} + \frac{\partial(VU)}{\partial X} + \frac{\partial(VV)}{\partial Y} = P_r \frac{\partial^2 V}{\partial X^2} + P_r \frac{\partial^2 V}{\partial Y^2} - \frac{\partial P}{\partial Y} + S_V \quad (3)$$

$$\frac{\partial \theta}{\partial \tau} + \frac{\partial(U\theta)}{\partial X} + \frac{\partial(V\theta)}{\partial Y} = \bar{\alpha} \frac{\partial^2 \theta}{\partial X^2} + \bar{\alpha} \frac{\partial^2 \theta}{\partial Y^2} + S_\theta \quad (4)$$

$$S_U = -\bar{C} \frac{(1-f_1)^2}{f_1^3 + b} U, \quad S_V = -\bar{C} \frac{(1-f_1)^2}{f_1^3 + b} V + R_a P_r \theta,$$

With,

$$S_\theta = \delta_1 ((\delta_2 - 1) \frac{1}{Ste} \frac{\partial f_1}{\partial \tau} + \frac{\delta_2}{3E_c L_c})$$

$$\delta_1 \begin{cases} 1 \text{ heat source} \\ 0 \text{ vertical walls} \end{cases}, \quad \delta_2 \begin{cases} 1 \text{ heat source} \\ 0 \text{ PCM} \end{cases},$$

– Boundary conditions

Adiabatic walls: $\frac{\partial \theta}{\partial \eta} \Big|_{wall} = 0, \quad \bar{\eta} \perp wall$

Interface wall–PCM:

$$\theta_s = \theta_m \quad \text{and} \quad K_m \frac{\partial \theta}{\partial X} \Big|_{X=0} = K_s \frac{\partial \theta}{\partial X} \Big|_{X=0}$$

Interface heat sources–PCM:

$$\theta_c = \theta_m \quad \text{and} \quad K_m \frac{\partial \theta}{\partial \eta} \Big| = K_c \frac{\partial \theta}{\partial \eta} \Big|$$

(η is the distance measured normal to the interface heat source - PCM interface)

– Initial conditions $\theta = U = V = f_1 = 0$

3. Results and discussion

Initially the PCM is solid and its temperature is equal to the melting temperature ($T_0 = T_m = 36 \text{ }^\circ\text{C}$). The geometrical parameters of the enclosure and heat sources are displayed in Table 1.

Table 1- Geometrical parameters (m)

E	l_c	γ	δ	l	e_s	w
0,001	0,005	0,005	0,0025	0,03	0,001	0,03

The control parameters other than the non-dimensional frequency are set at their following reference values.

$$Ra = 1.1461 \cdot 10^8, \quad Pr = 67.833, \quad Ste = 2.240, \quad l_0 = 0.0297m$$

$$\bar{\alpha}_c = 1465.58, \quad \bar{\alpha}_s = 70.55, \quad \bar{\alpha}_{m,s} = 1.0, \quad K_C = 2664.45$$

$$K_s = 130.90, \quad K_{m,s} = 1.0, \quad A = 1.0, \quad E_C = 0.033$$

$$L_C = 0.168, \quad E_s = 0.033, \quad \nabla = 0.084, \quad \Gamma = 0.168$$

3.1 Influence of the frequency of the pulsed power

Table 2 shows the different values of the frequency f (period P_e) of the pulsed power generated in each heat source. Note that the amount of heat provided by the heat sources for a period equal to the reference period ($P_{ref} = 310$ s, corresponding to a frequency $f_{ref} = 35.76$) is the same for all selected frequencies. Thus, one can search the optimal frequency that ensures better heat transfer for the same amount of heat provided by heat sources.

Table 2 - Dimensionless frequency values.

Dimensionless frequency	Dimensionless times τ_1 and τ_2 corresponding to the minimum and maximum values of the dimensionless power (corresponding to 10 and 50 (W/m), respectively)	Dimensionless period P_e
35,76	0,027 - 0,001 (300 s – 10 s)	0,028 (310 s)
71,53	0,0135 - 0,0005 (150 s – 5 s)	0,014 (155 s)
143,06	0,0067 - 0,00025 (75 s – 2,5 s)	0,007 (77,5 s)
286,13	0,00335 - 0,00012 (37,5 s – 1,25 s)	0,0035 (38,75 s)

Figure 3 displays the time wise variation of the dimensionless maximum temperature of the heat sources and liquid fraction for different dimensionless frequencies, the aspect ratio $A = 1$. The oscillations of the maximum dimensionless temperature are due to those of the generated power in the heat sources. It also appears from this figure that the oscillations are reduced with the increase of the dimensionless frequency of the power generated in the heat sources. Indeed, when the frequency is increased, the oscillation period is reduced. Thus, the heat sources do not have enough time to warm up. For each dimensionless frequency, the time evolution of the dimensionless maximum temperature is marked by three distinct regions. The first regime characterized by an increase in extreme values of the dimensionless maximum temperature versus time. This regime marks the beginning of the melting of PCM where the heat transfer by conduction is predominant. During this regime, the heat transfer in the liquid layer formed is essentially by conduction. The heat flux extracted by the

liquid PCM is not sufficient to prevent the increase of the maximum dimensionless temperature of heat sources. When the liquid becomes relatively wide area, a natural convective movement of the liquid PCM manifests and increases, therefore, the heat flow extracted from the heat sources. This is reflected in the evolution of the maximum dimensionless temperature which oscillates between two practically stable extreme values: it is the periodic regime. As the liquid layer expands, its dimensionless average temperature increases, and the heat discharged from the heat sources is reduced. This reduction leads to the increase in extreme values of the maximum dimensionless temperature of heat sources: this is the third regime. It should be noted that the increase in the dimensionless frequency is favorable for applications related to the cooling of electronic components. Indeed, and as explained above, an increase in the dimensionless frequency reduces maxima of the maximum dimensionless temperature. This has the effect of reducing the melting time. The temporal evolution of the liquid fraction is also given in the same figure. One can notice the slight improvement in the melting of the PCM with the increase in dimensionless frequency of the dimensionless generated power in the heat sources.

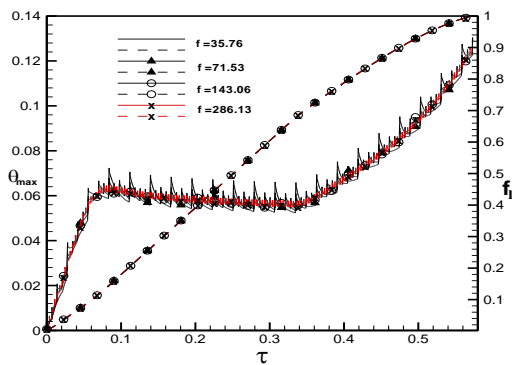


Fig. 3- The time wise variation of the dimensionless maximum temperature of the heat source (solid lines) and liquid fraction (dashed lines) for different dimensionless frequencies.

3.2 aspect ratio effect

Figure 4 shows the temporal variation of the maximum dimensionless temperature θ_{\max} , and the liquid fraction f , corresponding to the reference case (the reference frequency, $f_{\text{ref}} = 35.76$). As it can be seen from this figure, the time evolution of θ_{\max} goes through the same phases as those described in the previous section. The analysis of such a figure shows that the durations of the periodic regime and safe operation reduced when the aspect ratio decreases. It is necessary, too, to note that for low values of the aspect ratio, A , the PCM contained in the upper portion melts rapidly and the upper heat source quickly overheats. Thus, we conclude that the

cavities with high aspect ratios are a good solution for the cooling of electronic components.

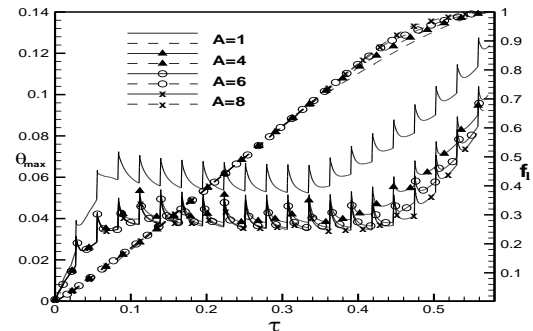


Fig. 4-Effect of the aspect ratio A on the time evolution of the dimensionless maximum temperature (solid lines) and the liquid fraction, f , (dashed lines).

4. Conclusion

Heat storage by melting in an MCP was modeled and analyzed. The main results cleared from this study can be summarized as follows:

- For each dimensionless frequency, the time evolution of the maximum dimensionless temperature heat sources is marked by three regimes;
- The increase of the frequency accelerates the overheating of heat sources;
- The cavities with high aspect ratios are a good solution for the cooling of electronic components;
- The cavities having a high aspect ratio is a practical solution for thermal energy storage and decreases the melting time;

References

- [1] H.H.-S. Chu, S.W. Churchill et C.V.S. Patterson, (1976). *The effect of heater size, location, aspect ratio, and boundary conditions on two-dimensional, laminar, natural convection in rectangular channels*, *J. Heat Transfer*, (98), 195-201.
- [2] Y. Zhang, Z. Chen, Q. Wang and Q. Wu (1993). *Melting in an enclosure with discrete heating at a constant rate*, *Experimental Thermal and Fluid Science*, (6), 196-201,
- [3] B. Binet et M. Lacroix, (1998). *Etude de la fusion dans des enceintes munies de sources de chaleur discrètes*, *Thèse de Doctorat (Philosophiae Doctor)*, Université de Sherbrooke (Québec), Canada,
- [4] Sh. Krishnan, V Garimella, (2004). *Analysis of a Phase Change Energy Storage System for Pulsed Power Dissipation*, *IEEE Transactions on Components and Packaging Technologies*, (27), 191-199.
- [5] M. Faraji, (2010). *Etude numérique des transferts de chaleur dans une enceinte confinant un matériau à changement de phase et chauffée par des sources de chaleur protubérantes sur une paroi conductrice verticale*, *Thèse de doctorat, Faculté des sciences Semlalia, Université Cadi Ayyad, Marrakech, Maroc*